Journal of Biomolecular Screening
2016, Vol. 21(5) 427–436

DOI: 10.1177/1087057115618348
jbx.sagepub.com
SAGE

A KNIME-Based Analysis of the Zebrafish Photomotor Response Clusters the Phenotypes of 14 Classes of Neuroactive Molecules

Daniëlle Copmans[1], Thorsten Meinl[2], Christian Dietz[3], Matthijs van Leeuwen[4], Julia Ortmann[5], Michael R. Berthold[3], and Peter A. M. de Witte[1]

Abstract

Recently, the photomotor response (PMR) of zebrafish embryos was reported as a robust behavior that is useful for high-throughput neuroactive drug discovery and mechanism prediction. Given the complexity of the PMR, there is a need for rapid and easy analysis of the behavioral data. In this study, we developed an automated analysis workflow using the KNIME Analytics Platform and made it freely accessible. This workflow allows us to simultaneously calculate a behavioral fingerprint for all analyzed compounds and to further process the data. Furthermore, to further characterize the potential of PMR for mechanism prediction, we performed PMR analysis of 767 neuroactive compounds covering 14 different receptor classes using the KNIME workflow. We observed a true positive rate of 25% and a false negative rate of 75% in our screening conditions. Among the true positives, all receptor classes were represented, thereby confirming the utility of the PMR assay to identify a broad range of neuroactive molecules. By hierarchical clustering of the behavioral fingerprints, different phenotypical clusters were observed that suggest the utility of PMR for mechanism prediction for adrenergics, dopaminergics, serotonergics, metabotropic glutamatergics, opioids, and ion channel ligands.

Keywords

zebrafish, neuroactive drug discovery, photomotor response, data analysis, KNIME

Introduction

In 2010, the photomotor response (PMR) of zebrafish embryos was reported for the first time as a robust behavior that allows high-throughput neuroactive drug discovery.[1] This study by Kokel and colleagues thoroughly characterized the PMR as a stereotypic series of motor behaviors by zebrafish embryos in response to high-intensity light pulses. The potential of a PMR-based behavioral assay was demonstrated in a chemical screen of 14,000 small molecules, identifying hundreds of PMR-modifying hits. As PMR is regulated by multiple neurotransmitter pathways, PMR-modifying molecules are considered to be neuroactive. Interestingly, PMR behavior was also proven to allow target identification of novel hits by co-clustering of molecules with similar phenotypes and with known mechanism of action (MOA).[1] This characteristic of PMR can have a broad applicability when generating a large reference map of PMR phenotypes of small molecules with known MOA. Then, the MOA of an interesting hit or drug candidate can be predicted by co-clustering and a targeted approach of mechanistic investigation can be done. However, little is known about the predictive value of PMR phenotyping.

[1]Laboratory for Molecular Biodiscovery, Department of Pharmaceutical and Pharmacological Sciences, KU Leuven, Leuven, Belgium
[2]KNIME.com AG, Zurich, Switzerland
[3]Chair for Bioinformatics and Information Mining, Department of Computer and Information Science, University of Konstanz, Konstanz, Germany
[4]Machine Learning Group, Department of Computer Science, KU Leuven, Leuven, Belgium
[5]Department of Bioanalytical Ecotoxicology, Helmholtz Centre for Environmental Research, UFZ, Leipzig, Germany

Received Aug 14, 2015, and in revised form Oct 19, 2015. Accepted for publication Oct 29, 2015.

Supplementary material for this article is available on the *Journal of Biomolecular Screening* Web site at http://jbx.sagepub.com/supplemental.

Corresponding Author:
Peter A. M. de Witte, Laboratory for Molecular Biodiscovery, Department of Pharmaceutical and Pharmacological Sciences, KU Leuven, Herestraat 49 bus 824, 3000 Leuven, Belgium.
Email: peter.dewitte@pharm.kuleuven.be

Which neurological pathways can modify the PMR in a robust and distinct manner has only been characterized in part, and there has been no characterization of pathways that cannot. There has also been no characterization of the rate of false negatives. Thus, there is a need to further characterize the predictive value of the PMR.

PMR is a very complex behavior to analyze, and data are generated rapidly by video recording. Motion is recorded as a change in pixels continuously in time for 30 s for each well of a 96-well plate. In our setup, a time frame of 0.067 s was used. This implies that for each well, 448 data points are generated in 30 s. As replicate wells are used per condition and in case of screening, hundreds—up to thousands—of molecules are analyzed, an excess of data is rapidly generated. For example, this study resulted in more than 1.5 million data points for the analysis of only 767 compounds. Hence, there is a need for rapid and easy analysis of the behavioral data.

In this study, we developed an automated workflow for PMR analysis using the KNIME Analytics Platform (http://www.knime.org).[2] This is an open-source integration platform providing a powerful and flexible workflow system combined with data analytics, visualization, and reporting capabilities. KNIME integrates nodes for machine learning, statistical data analysis, and interfaces to various scripting languages, for example, the statistical programming language R. KNIME's functionality can be extended with nodes provided via an online repository (the so-called KNIME extensions). Our automated analysis workflow allows simultaneous calculation of a behavioral fingerprint for all analyzed molecules and further processing of the data, for example, by hierarchical clustering. Since the workflow has broad utility for behavioral analysis, it is made freely accessible on the KNIME Public Example Server as 050_Applications/050021_PMR Analysis.

Furthermore, to further characterize the potential of the PMR for mechanism prediction, we performed PMR analysis of 767 neuroactive compounds covering 14 different receptor classes (adrenergics, dopaminergics, serotonergics, opioids, sigma ligands, cholinergics, histaminergics, melatonin ligands, ionotropic glutamatergics, metabotropic glutamatergics, GABAergics, purinergics, adenosines, and ion channel ligands) using the KNIME workflow. Our results confirm the utility of the PMR assay to identify a broad range of neuroactive molecules. Moreover, the observations suggest that PMR can be useful for mechanism prediction for adrenergics, dopaminergics, serotonergics, metabotropic glutamatergics, opioids, and ion channel ligands.

Materials and Methods

Zebrafish Maintenance

Adult zebrafish (*Danio rerio*) stocks of the AB strain (Zebrafish International Resource Center, Eugene, OR) were maintained at 28.0 °C, on a 14/10 h light/dark cycle under standard aquaculture conditions. Fertilized eggs were collected via natural spawning. Embryos and larvae were kept on a 14/10 h light/dark cycle in embryo medium: 1.5 mM HEPES, pH 7.6, 17.4 mM NaCl, 0.21 mM KCl, 0.12 mM $MgSO_4$, and 0.18 mM $Ca(NO_3)_2$ in an incubator at 28.0 °C. All zebrafish experiments carried out were approved by the Ethics Committee of the University of Leuven (Ethische Commissie van de KU Leuven, approval no. P101/2010) and by the Belgian Federal Department of Public Health, Food Safety and Environment (Federale Overheidsdienst Volksgezondheid, Veiligheid van de Voedselketen en Leefmilieu, approval no. LA1210199).

Compound Libraries and Compounds

A total of 633 compounds from the Screen-Well Neurotransmitter Library (BML-2810-0100, Enzo Life Sciences, Farmingdale, NY), 71 compounds from the Screen-Well Ion Channel Ligand Library (BML-2805-0100, Enzo Life Sciences), 33 selected compounds from the Spectrum Collection Library (MicroSource Discovery Systems, Inc., Gaylordsville, CT), and 30 individually purchased compounds (Sigma-Aldrich, Prestwick, St. Louis, MO) were analyzed by the PMR assay. Positive controls isoproterenol and apomorphine were purchased from Sigma-Aldrich, and diazepam was obtained from the pharmacy (Roche, Basel, Switzerland; valium 10 mg/2 mL ampullas).

Compound Preparation

Isoproterenol, diazepam, and apomorphine were dissolved in DMSO to 10, 5, 2.5, and 1.25 mM concentrations and 100-fold diluted in the embryo's swimming water (embryo medium) to final concentrations of 100, 50, 25, and 12.5 μM with a final solvent concentration of 1% DMSO. A total of 767 compounds were analyzed by the PMR assay at a concentration of 50 μM with a final solvent concentration of 0.5% or 1% DMSO. A total of 737 compounds were provided by compound libraries as 10 mM DMSO stocks (water was used as a solvent for DMSO insoluble compounds) and 200-fold diluted in the embryo's swimming water to final concentrations of 50 μM (0.5% DMSO). Thirty individually purchased compounds were prepared as 5 mM DMSO stocks and 100-fold diluted in the embryo's swimming water to final concentrations of 50 μM (1% DMSO). Vehicle (VHC)-treated controls were treated with 0.5% DMSO, 1% DMSO, or water in accordance with the final solvent concentration of the analyzed compounds.

Photomotor Response Assay

Protocol was adapted from Kokel and colleagues.[1] The photomotor response of zebrafish embryos was investigated by automated behavioral tracking (Zebrabox, ViewPoint,

Lyon, France) at 30–32 h postfertilization (hpf). Zebrafish embryos were placed in a 96-well plate in embryo medium at 27–29 hpf (prim-15 stage), followed by a dark incubation of 3 h with VHC or compound prior to tracking, including 20 min of habituation in the Zebrabox chamber. Concurrent controls were run with each compound to avoid interplate variation. Exactly five embryos were placed per well to obtain a cumulative photomotor response. Total motion was recorded for 30 s at 15 frames per second (fps) in fully dark conditions with a high-intensity light pulse (5.2 mW/cm^2, 38,000 lux) given at 10 and 20 s lasting 1 s. Raw data of total movement per well were used and are defined as the sum of all image pixel changes detected during the time interval of 0.067 s, corresponding to one frame. Total motion was plotted in function of time, and average motion was plotted per time period. The PMR was divided into eight time periods. The so-called prestimulus phase, at which embryos show basal activity, was considered one time period (PRE, seconds 0–10). The latency phase, which occurs immediately after the first light stimulus, was considered one period (L, seconds 10–11). The excitatory phase, at which embryos shake vigorously, was divided into three periods (E1, seconds 11–13; E2, seconds 13–16; E3, seconds 16–20). Finally, the refractory phase, at which embryos show a lower-than-basal activity, is triggered by the second light stimulus and was divided into three periods as well (R1, seconds 20–22; R2, seconds 22–25; R3, seconds 25–30). For control experiments with isoproterenol, diazepam, and apomorphine, data were pooled from three independent experiments with four to six replicate wells per condition. For screening of neuroactive molecules, data were pooled from three or six replicate wells per molecule. Replicate wells were scattered over the 96-well plate. The PMR assay was standardized for temperature at 28 °C, including habituation and behavioral tracking in the Zebrabox, which was placed in an incubator for temperature control. Automated behavioral tracking was standardized for light intensity by the usage of only the 30 central wells of a 96-well plate, ensuring identical light intensity regardless of the position.

Microscopic Evaluation of Toxicity

The PMR assay was immediately followed by visual evaluation of the embryos by a light microscope to assess toxicity of pharmacological treatment. Overall morphology, heartbeat, and touch response were investigated. Overall morphology was considered normal in case of a normal appearance. Overall morphology was considered abnormal in case of signs of necrosis, which was especially seen at the tip of the tail. We did not encounter other morphological abnormalities such as edema or developmental defects. The heartbeat was considered normal, reduced, or absent. The behavioral response of embryos to touch was investigated by touching the chorion of the embryo at the site of the yolk with a bold needle. Touch response was considered normal (including hyperactivity), reduced, or absent. Compounds were scored as normal (N) if exposed embryos had a normal morphology, heartbeat, and touch response. Compounds were scored as sedative (S) if exposed embryos had a normal morphology, normal or reduced heartbeat, and a reduced or absent touch response. Compounds were scored as toxic (T) if exposed embryos had an abnormal morphology or an absent touch response with absence of heartbeat.

Behavioral Fingerprints

Behavioral fingerprints were calculated by an automated workflow using KNIME Analytics Platform 2.11.3. A behavioral fingerprint represents the embryonic motion during the eight PMR periods by subsequent numeric values. Each period was described by the first (25% of motion, Q1) and third (75% of motion, Q3) quantile, giving a total of 16 numeric values. For comparison with VHC-treated embryos, pseudo Z-scores were calculated for each log-transformed quantile by the following formula:

$$\text{pseudo Z} - \text{score} = \frac{\mu_{treatment} - \mu_{control}}{\sigma_{control}}$$

The mean value (μ) of the control condition is subtracted from the mean value of the treatment condition, and the result is divided by the standard deviation (σ) of the control condition to obtain the pseudo Z-score. The behavioral fingerprints consist of 16 subsequent pseudo Z-scores, calculated from the Q1 and Q3 from each PMR period. The definition and calculation of behavioral fingerprints or barcodes are adapted from Kokel and colleagues.[1,3]

KNIME Analytics Platform

Supplemental Figure S1 shows the main window of the KNIME Analytics Platform. On the left, the "KNIME Explorer" shows the available workflows. The "Node Repository" contains the available nodes. In the center, an open workflow is shown. A description of the selected node is given at the right of the window. The "Console" is seen at the bottom, which gives details about warnings and errors that occurred during workflow execution (**Suppl. Fig. S1**).

A KNIME workflow is composed of multiple nodes that are connected by ports. Data are passed along the connections between ports in a table structure with columns (each having a certain type) and rows. The parameters of nodes and their documentation are available via a configuration dialog. More complex workflows, such as the one we developed and describe below, also contain loops and switches. Loops allow applying the same series of nodes to multiple input files one at a time, and switches allow executing only

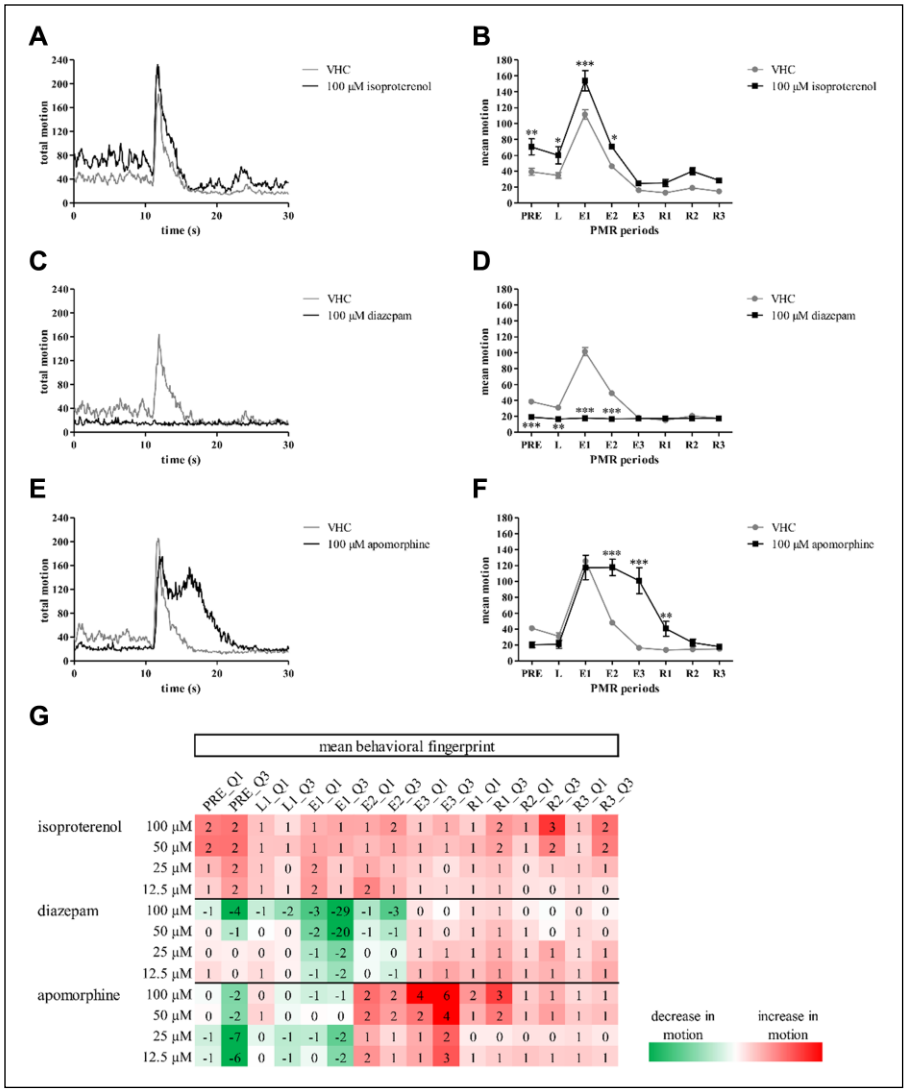

Figure 1. PMR of 30–32 hpf zebrafish embryos incubated with positive controls isoproterenol, diazepam, and apomorphine. Embryos were treated for 3 h with vehicle (VHC) or drug. (**A-F**) Total motion and mean motion of embryos treated with VHC or 100 µM of drug. (**A, C, E**) Total motion of the embryos as a function of time. (**B, D, F**) Mean motion of the embryos as a function of eight PMR periods. (**G**) Mean behavioral fingerprints of embryos treated with 12.5, 25, 50, and 100 µM of isoproterenol, diazepam, and apomorphine, respectively. (**B, D, F**) Data are expressed as mean ± SEM. Statistical analysis was done by two-way ANOVA (GraphPad Prism 5). Significance levels: *$p < 0.05$, **$p < 0.01$, ***$p < 0.001$.

certain branches of the workflow based on user-defined conditions. To further structure a workflow, KNIME provides the so-called metanodes to group a collection of nodes. Grouping into metanodes can be used to hide a complex series of nodes and instead provide a high-level view on the data flow.

Results

PMR Analysis of Positive Controls Isoproterenol, Diazepam, and Apomorphine

To validate our optimized PMR assay, three drugs with known PMR-modifying effects were analyzed: isoproterenol, diazepam, and apomorphine. These drugs were earlier shown by Kokel and colleagues to cause excitation, inhibition, and latency of the excitatory phase, respectively.[1]

Embryos incubated for 3 h with 100 µM isoproterenol demonstrated an overall excitation of the photomotor response in comparison with VHC-treated controls. This increase in motion was observed to be significant at the prestimulus phase ($p < 0.01$), latency phase ($p < 0.05$), and first ($p < 0.001$) and second ($p < 0.05$) excitation periods (**Fig. 1A,B**). Embryos incubated for 3 h with 100 µM diazepam demonstrated an overall inhibition of the PMR in comparison with VHC-treated controls. This decrease in motion was observed to be significant at the prestimulus phase ($p < 0.001$), latency phase ($p < 0.01$), and first ($p < 0.001$) and second ($p < 0.001$) excitation periods (**Fig. 1C,D**). Finally, embryos incubated for 3 h with 100 µM apomorphine demonstrated a complex altered PMR in comparison to VHC-treated embryos. The PRE motion was lowered, no difference was seen in the E1 period, and a significant increase in motion was observed for the E2 ($p < 0.001$), E3

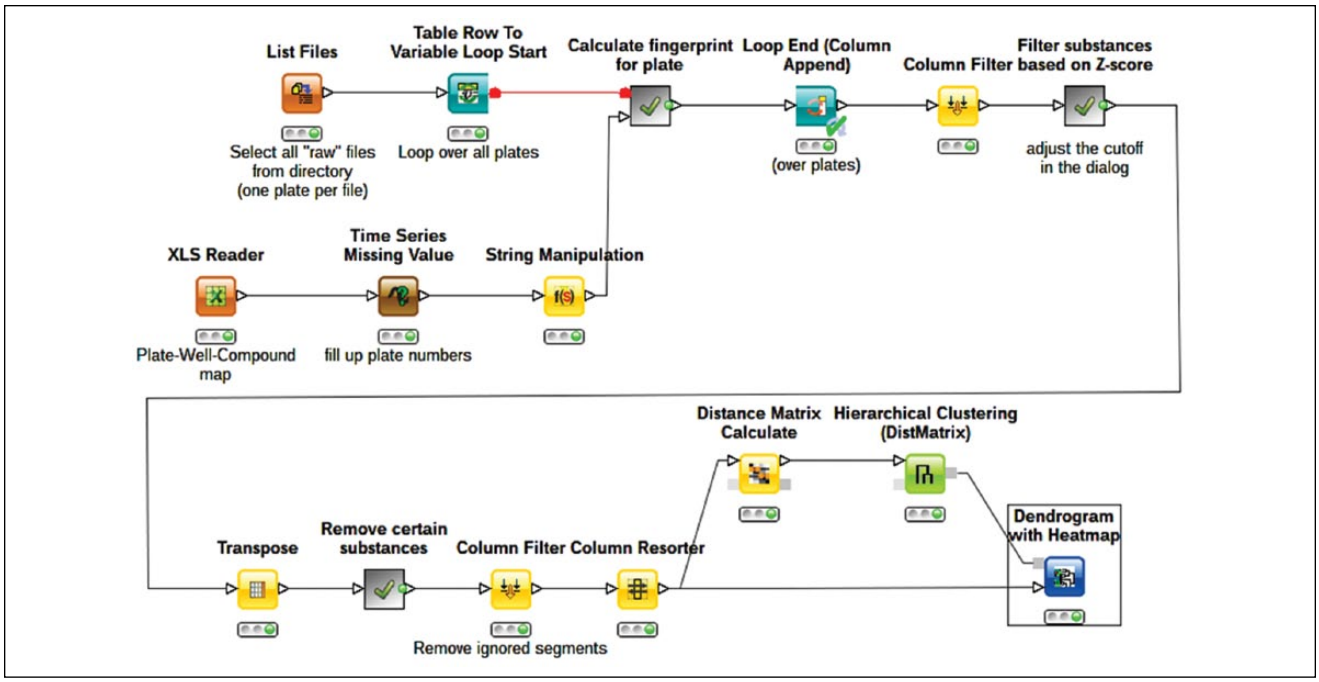

Figure 2. KNIME workflow for PMR analysis. The workflow structure is using metanodes in order to make it more readable and easier to maintain.

($p < 0.001$), and R1 ($p < 0.01$) periods. These latter observations were due to the occurrence of a second excitation peak, delayed to the incidence of the first excitation peak. This excitation peak only slowly passed in comparison with the normal excitation peak of control embryos (**Fig. 1E,F**). Concentration dependency was observed for all phenotypes (**Fig. 1G**). Taken together, these observations suggest that our PMR assay can detect PMR-modifying effects very similar to those reported by Kokel and colleagues.

Generation of an Automated KNIME Workflow for Large-Scale PMR Analysis

For our large-scale PMR analysis of neuroactive molecules, behavioral analysis had to be rapid, easy, and automated. Therefore, a KNIME workflow was built to analyze the data recorded by the Zebrabox. It computes the pseudo Z-scores and behavioral fingerprints for each molecule, and finally performs hierarchical clustering of the pseudo Z-scores and generates a dendrogram. The workflow is rather complex, as it performs all steps, from reading the raw data until the final dendrogram. In order to make it more readable, it has been divided into several sections using the metanode concept mentioned in Materials and Methods. The workflow is shown in **Figure 2**. For reasons of space, we will only highlight the important parts. The complete workflow, including inline comments, can be downloaded from KNIME's Public Example Server directly from within KNIME (login via the entry in the "KNIME Explorer" view).

The workflow requires two types of input. The first input is the raw data, which consists of several CSV files (one per 96-well plate) containing raw measurements for all wells on the plate over the 30 s interval (about 28,000 rows per file). The data are divided into three columns: time, well ID (e.g., c1 and c2), and embryonic motion measurement. The workflow iterates over all files in the experiment's directory and computes the behavioral fingerprint for each molecule (see below). The second input is a file that contains a mapping between the plates/wells and the treatment in each well (referred to as substance in the workflow), for example, VHC or a certain molecule. Additionally, it may contain manual annotations, indicating whether a well should be ignored in the further analysis, for example, because the well was empty or no treatment was added.

Computation of the behavioral fingerprints inside the "Calculate fingerprint" metanode works as follows (**Fig. 3A**). First, the raw input data are transformed from the three-column structure described above into a table with a column for each well and a row for each time point ("Data Transformation" metanode). The values in the cells are the measurements. The "Unify Domains" metanode ensures that the y axes in the line plots have the same scales and can therefore be directly compared. **Figure 3B** shows some plots generated by the "Line Plots" metanode. The Numeric Binner assigns names to the time intervals ("segments") as described above (e.g., L, E1, and R1). The "Group Loop" iterates over the measurements in each of the segments separately. For each well/substance in each segment, we compute the 25% and 75% quantiles (Q1

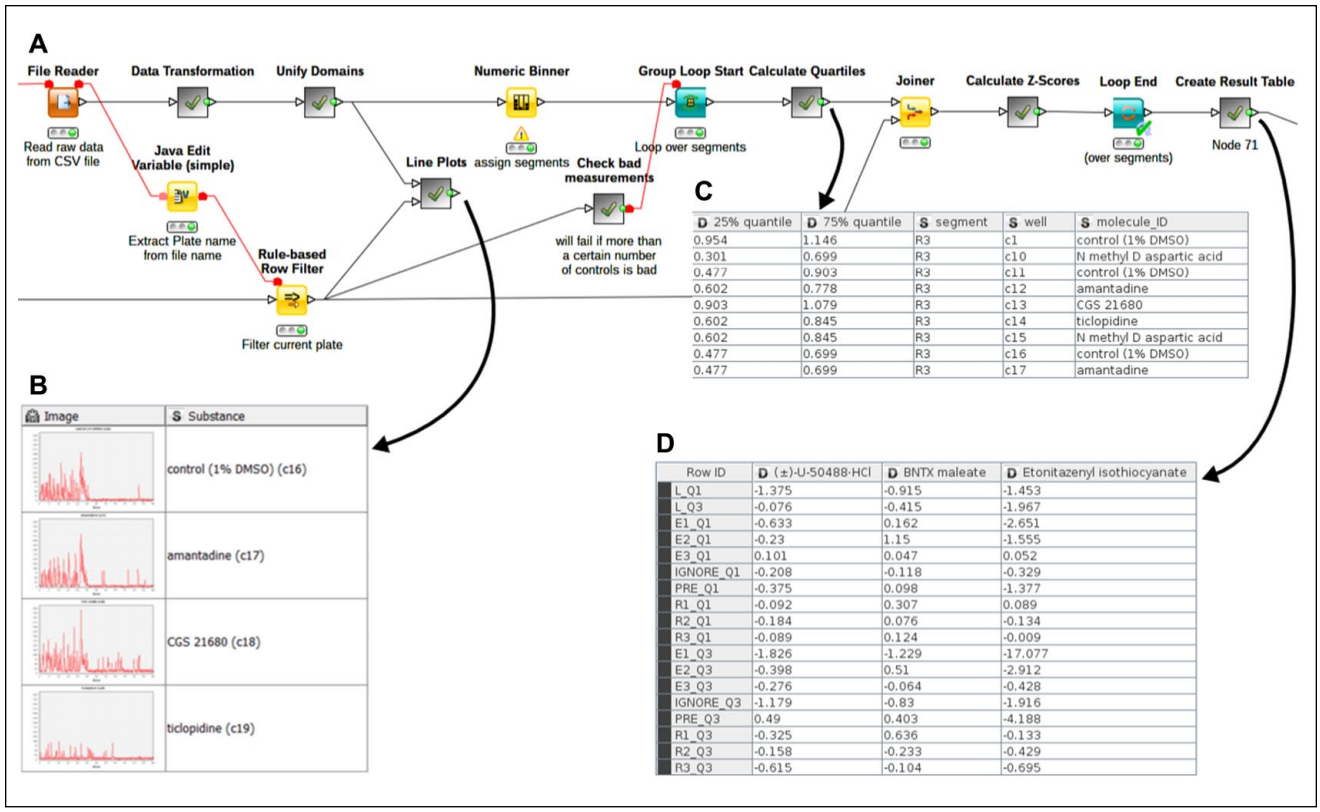

Figure 3. A detailed view of the metanode that computes the behavioral fingerprints. (**A**) Inside view of the metanode "Calculate fingerprint for plate". The metanode is again divided into several nested metanodes. (**B**) Result table of the metanode "Line Plots". Line plots show the embryonic motion in time in a certain well. (**C**) Result table of the metanode "Calculate Quartiles" showing some computed quantiles for segment R3. (**D**) Final result table showing the pseudo Z-scores for tested molecules.

and Q3, respectively) and use the logarithms of these values in subsequent steps ("Calculate Quartiles" metanode). **Figure 3C** shows parts of the resulting table for segment R3. Finally, we compute the pseudo Z-scores based on the quartiles of the controls and the molecules, and transform the structure to obtain a row for each segment and a pseudo Z-score (Q1 and Q3) with the corresponding values for each molecule in the columns (**Fig. 3D**). This is the result of the outermost loop, which completes the computation of all values for all plates. Note also the "Check bad measurements" metanode in the center of **Figure 3A**. This node provides an extra internal control to avoid the analysis of a plate when multiple control wells are ignored due to an error, for example, a software error or manual error. It checks the manual annotations for all wells, and if such a plate occurs, it fails and will stop execution of the remaining workflow.

The next step is to remove all columns/molecules with pseudo Z-scores below a certain threshold. The threshold can easily be set by the user via the configuration dialog of the "Filter substances" metanode, without having to know the other details of the filtering.

In the bottom part of the main workflow (**Fig. 2**), we first transpose the table so that each molecule is in a row and the pseudo Z-scores for the segments are in the columns. Next, we remove the segment "IGNORE" that represents seconds just before and after the 30 s PMR period that are not taken into account. Then we compute a distance matrix (Euclidean distance) using the pseudo Z-scores as dimensions and perform hierarchical clustering with complete linkage. The final result is a dendrogram, including a heatmap, as shown in **Figure 4** and discussed in the next sections.

PMR Analysis of 14 Classes of Neuroactive Molecules

A systematic analysis was done of 767 neuroactive molecules covering 14 different receptor classes (adrenergics, dopaminergics, serotonergics, opioids, sigma ligands, cholinergics, histaminergics, melatonin ligands, ionotropic glutamatergics, metabotropic glutamatergics, GABAergics, purinergics, adenosines, and ion channel ligands) to further characterize the neurological pathways that can alter PMR. Embryos were incubated either with vehicle (0.5 or 1% DMSO) or with 50 µM of a certain molecule (final solvent concentration of 0.5 or 1% DMSO) for 3 h prior to PMR analysis. PMR analysis was followed by microscopic evaluation of embryo morphology,

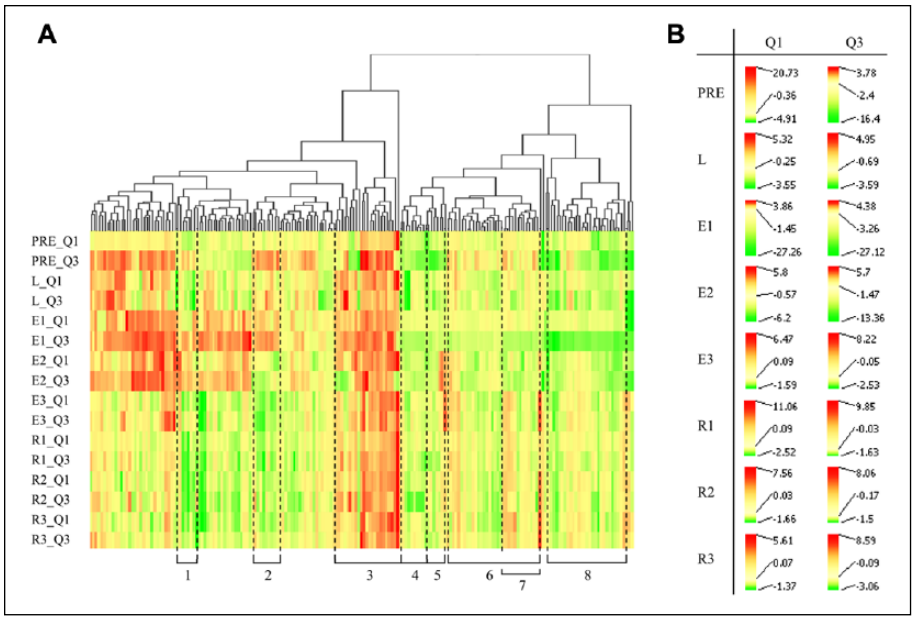

Figure 4. Hierarchical clustering of PMR positive molecules. Behavioral fingerprints of PMR positive molecules were clustered by complete linkage of the distance matrix (Euclidean distance). (**A**) Heatmap and dendrogram are shown. Numbers 1–8 indicate clusters that are enriched with molecules from a single receptor class. (**B**) Color scales of the heatmap are given for the first (Q1) and third (Q3) quantiles for all PMR periods. PRE, prestimulus phase; L, latency phase; E1, excitatory period 1; E2, excitatory period 2; E3, excitatory period 3; R1, refractory period 1; R2, refractory period 2; R3, refractory period 3.

Table 1. PMR Analysis of Neuroactive Compounds.

	Number of Molecules	Rate (%)	
Total	767		
Normal (N)	724	94.4	
Sedative (S)	26	3.4	
Toxic (T)	17	2.2	Toxicity rate
Pseudo Z-score ≥ |2|			
Positives	324	42.2	True positive rate
Negatives	443	57.8	False negative rate
Pseudo Z-score ≥ |3|			
Positives	195	25.4	True positive rate
Negatives	572	74.6	False negative rate
Pseudo Z-score ≥ |5|			
Positives	117	15.3	True positive rate
Negatives	650	84.7	False negative rate

heartbeat, and touch response, to assess toxicity of pharmacological treatment. A low rate of sedative (3.4%) and toxic (2.2%) compounds was observed, suggesting that 50 µM of most neuroactive compounds is well tolerated by zebrafish embryos during an acute exposure (**Table 1**).

A PMR positive molecule was defined as a molecule that modifies the photomotor response such that its behavioral fingerprint contains at least one pseudo Z-score with an absolute value exceeding 3. At this critical value, 195 molecules were observed to be PMR positive, giving a true positive rate of 25.4% and a false negative rate of 74.6%. Thus, 25.4% of known neuroactive molecules alter PMR sufficiently at the analyzed concentration to be identified as neuroactive by the PMR assay. At a lower critical value of 2, 324 molecules were PMR positive, giving a true positive rate of 42.2% and a false negative rate of 57.8%. This lower stringency allows the detection of more than 40% of the neuroactive molecules at 50 µM. At a higher critical value of 5, 117 molecules were still observed to be positive, giving a true positive rate of 15.3% and a false negative rate of 84.7% (**Table 1**). These PMR positives alter the PMR so much that a difference in motion of at least five times the standard deviation of the control is seen. For further analysis, the critical value of 3 was taken to consider only neuroactive molecules that alter PMR in a robust manner.

Among PMR positive molecules, all neurological pathways are represented as molecules from all receptor classes were included. This observation confirms the utility of PMR to detect a broad range of neuroactive molecules and suggests the involvement of these pathways in PMR regulation.

Hierarchical Clustering of PMR Positive Molecules

To characterize the classes of neuroactive molecules that can induce a distinct PMR phenotype, hierarchical clustering of behavioral fingerprints of the 195 PMR positive molecules was done (**Fig. 4**). A cluster was considered to be enriched with molecules from a certain neurological pathway if more than one-third of the molecules belong to a single receptor class and the cluster has a minimum size of seven fingerprints. This was determined in a top-down

approach evaluating the 30 most distinct clusters of the heatmap, as indicated by the workflow. Eight clusters were observed to be enriched with a certain class of molecules. These clusters are indicated by numbers 1–8 in **Figure 4**.

Cluster 1 is enriched with behavioral fingerprints from opioids. Five out of seven molecules are opioid receptor ligands. These show a higher activity in the E1 and E2 period in comparison to control behavior and a reduced activity in periods E3, R1, R2, and R3 (cluster 1; **Suppl. Fig. S2**). Cluster 2 is enriched with ligands from metabotropic glutamatergic receptors. Four out of 10 molecules belong to this class of receptors; 3 of them are receptor agonists. These molecules show a behavioral fingerprint with decreased activity mainly in periods E2 and E3, but also in R1–R3 (cluster 2; **Suppl. Fig. S2**). Cluster 4 is also enriched with ligands from metabotropic glutamatergic receptors, but all are receptor antagonists. Four out of nine molecules belong to this class of receptors and show a reduced activity, especially in the PRE, E1, and E2 periods, in comparison to controls (cluster 4; **Suppl. Fig. S2**). Three of these molecules have the mGlu5 receptor as target. Cluster 3 is enriched with ligands from adrenergic receptors. Ten out of 23 molecules belong to this class of receptors; 8 of them are receptor agonists and 7 molecules are α receptor ligands. They show a behavioral fingerprint with an overall increased activity in comparison to controls (cluster 3; **Suppl. Fig. S2**). Cluster 5 is enriched with ligands from dopaminergic receptors. Six out of eight molecules belong to this receptor class; five of them are receptor agonists. Their behavioral fingerprints show a decreased activity, especially in the PRE and E1 phases (cluster 5; **Suppl. Fig. S2**). Cluster 8 is also enriched with ligands from dopaminergic receptors. Eleven out of 29 molecules belong to this class of receptors, both agonists and antagonists. Six of them are D4 receptor ligands. Their behavioral fingerprints also show a decreased activity in the PRE phase, but in comparison to cluster 5, the activity in the E1 period is much more decreased (cluster 8; **Suppl. Fig. S2**). Cluster 6 is enriched with behavioral fingerprints from different types of ion channel ligands. Twelve out of 33 molecules belong to this type of ligands, and 8 of them act on calcium channels. Their behavioral fingerprints show a decreased motion during the E1 and E2 periods and a moderate decrease or increase in motion in periods E3-R3 (cluster 6; **Suppl. Fig. S2**). Finally, cluster 7 is part of cluster 6. This smaller cluster is also enriched with ligands from serotonergic receptors. Five out of 13 molecules belong to this receptor class. Their behavioral fingerprints are very similar to those from cluster 6, but this subset shows a more decreased activity in the E1 and E2 periods (cluster 7; **Suppl. Fig. S2**).

In summary, ligands from the following classes of receptors were observed to induce a distinct PMR phenotype: adrenergics, dopaminergics, serotonergics, metabotropic glutamatergics, opioids, and ion channel ligands. This means that sigma ligands, cholinergics, histaminergics, melatonin ligands, ionotropic glutamatergics, GABAergics, purinergics, and adenosines seem to fail to induce a distinct PMR phenotype despite their strong PMR-modifying effects. These data suggest that PMR is useful for mechanism prediction only within the above first mentioned neurological pathways.

Discussion

With this study, a systematic PMR analysis was done of the different neurological pathways by analysis of 767 ligands that cover 14 receptor classes. Our results confirm the utility of the PMR assay to identify a broad range of neuroactive molecules, as was demonstrated by Kokel and colleagues.[1] The use of the PMR for mechanism prediction was further investigated and is suggested to be limited to adrenergics, dopaminergics, serotonergics, metabotropic glutamatergics, opioids, and ion channel ligands. Our data thereby confirm the study by Kokel and colleagues, who also reported phenotypical clusters for adrenergic and dopaminergic agonists.[1] Furthermore, we expand their findings with the report of distinct phenotypical clusters for serotonergics, metabotropic glutamatergics, opioids, and ion channel ligands. In contrast to the study by Kokel, we did not identify a cluster enriched with adenosine receptor antagonists. This is likely due to differences in protocol, for example, incubation time (3 h vs. 2–10 h), but can also be due to the more sensitive detection of embryonic motion by our setup (detection of motion in the entire well vs. detection of motion at six lines covering the well).

The identification of phenotypic clusters from adrenergics, dopaminergics, serotonergics, metabotropic glutamatergics, opioids, and ion channel ligands suggests that within these classes new molecules can be identified and the mechanism can be predicted by phenotypic similarity. This allows the use of PMR not only to screen for neuroactivity in general, but also to screen for a certain class of ligands, indicating their potential therapeutic use. Our data suggest that this is not possible for all neurological pathways, but is limited to the receptor classes mentioned above. Concerning the detail of mechanism prediction, an indication for agonistic or antagonistic activity is clear in four of the eight clusters, but an indication for a specific target or receptor is not so common. In our data set, only four targets were highly present in their respective clusters, that is, the mGlu5 receptor, α receptor, calcium channel, and D4 receptor. This is not surprising, as the annotated activity of a molecule will not always reflect its activity on the zebrafish target. This is due to possible differences between zebrafish and human receptors and is referred to as the zebrafish annotation problem.[4] Nevertheless, PMR phenotyping can be used for target prediction when screening for molecules without a predefined target. This is suggested by our data

and was already demonstrated by Kokel and colleagues, who identified novel acetylcholinesterase inhibitors by phenotypic similarity.[1]

The absence of phenotypic clusters from the other classes of ligands is due to the absence of distinct PMR phenotypes for each class and can have multiple causes. First, ligands from different classes can (in)directly affect the same PMR-regulating neurological pathway or affect different neurological pathways with a similar PMR-modifying effect. Second, there can be a large variation between ligands from the same receptor class in terms of conservation of the drug target in zebrafish, optimal test concentration, or drug absorption, which all can result in different PMR phenotypes. Third, as many neuroactive ligands have multiple targets, it is possible that these ligands do not induce a similar PMR phenotype within a certain class.

Furthermore, we observed a high false negative rate for PMR analysis at the analyzed concentration of 50 μM and after an acute exposure of 3 h. Analysis of multiple concentrations and exposure times will increase the number of true positives, but this will also largely reduce the throughput. Moreover, as many neuroactive drugs act on multiple targets, it can be expected to detect less specific behavioral fingerprints when analyzing compounds at high concentrations. Therefore, ideally, a concentration–response analysis should be performed for each compound to allow improved clustering of the fingerprints based on cross-concentration behavioral similarities within receptor classes. Such an approach not only would reduce the false negative rate, but also could improve phenotype-based mechanism prediction. Besides the analysis of compounds at a single concentration and exposure time, other causes for the observation of false negatives in this study could be malabsorption of the drug, failure of the immature metabolism to activate prodrugs, absence of the functional target in zebrafish or in the immature brain, or the drug target not being involved in PMR regulation.

For improved understanding of our results, it is important to know which neurological pathways are present in the immature brain of the zebrafish embryo. The PMR occurs between 30 and 40 hpf, while the light-evoked refractory phase is already observed from 27 hpf onward.[5] At these stages, primary neurogenesis is ongoing until 48 hpf, when secondary neurogenesis initiates. Primary neurogenesis involves the transient establishment of an early sensorimotor circuit that allows motor behaviors. These neurons were reported to include glutamatergic, GABAergic, cholinergic, and glycinergic neurotransmission at 24 hpf.[6–8] Furthermore, spatiotemporal expression of aminergic innervation in the developing zebrafish embryo demonstrated dopaminergic, (nor)adrenergic, and serotonergic neurotransmission at 24 hpf. Adrenergic or noradrenergic neurons were observed in the hindbrain in the developing locus coeruleus and also by 36 hpf in the medulla oblongata. Dopaminergic neurons were also observed in the locus coeruleus and furthermore in the posterior tuberculum that is localized in the diencephalon (forebrain). Serotonergic neurons were also observed in the posterior tuberculum and by 32 hpf in the spinal cord as well.[9,10] Finally, spatiotemporal expression of the zebrafish opioid receptors shows a wide distribution in the central nervous system at 24 and 48 hpf.[11,12] The early establishment of the main neurotransmission systems before and by the time of PMR initiation is in accordance with the phenotypical clusters we could detect. Moreover, the early aminergic innervation of the spinal cord by the hindbrain, which is described in a study by McLean and Fetcho,[9] is in line with the sudden shift in motor behavior from low-frequency touch responses until 26 hpf to high-frequency swimming from 28 hpf onward.[8] This swimming behavior is involved in the PMR and was shown to be driven by photosensitive hindbrain neurons.[5]

Expression studies have also demonstrated the early presence of adenosine,[13] purinergic,[14,15] and melatonin[16] receptors in the central nervous system of the developing zebrafish embryo at 24 hpf. This is in line with the identification of multiple PMR positive molecules from these receptor classes. We also identified PMR positive molecules that act through histamine or sigma receptors, suggesting their functionality at these early stages. The presence of these receptors in the central nervous system at 30 hpf has not yet been reported, to our knowledge, as only few studies have been done that did not include spatiotemporal investigations at this early stage.[17–19]

Furthermore, with this study a KNIME workflow was built to analyze behavioral data in a rapid and easy manner. The workflow is designed to calculate behavioral fingerprints for hundreds—up to thousands—of treatments at the same time, and finally to hierarchically cluster these fingerprints. This workflow enables everyone, without the need for programming skills or IT experience, to analyze behavioral data. Parameters can easily be changed through the configuration button of each node; for example, the type of distance measure, the type of linkage, and the critical pseudo Z-score value can be changed. Moreover, the workflow is designed such that nodes can easily be removed, added, or changed to alter the type of analysis.

Finally, in this study we focused on the applicability of the photomotor response, which is a nonvisual light-driven behavioral response. Other types of behavioral responses to neuronal stimuli can also be used for neuroactive drug discovery, for example, visual light-driven responses and auditory responses. One example is the automated rest/wake behavioral assay that was reported by Rihel and colleagues for phenotype-based target prediction and drug discovery.[20] The challenge becomes to correlate these different types of neuronal responses in drug screening strategies. One possibility is to generate a battery of different behavioral assays and combine the results as different bars within a

descriptive barcode. Such an approach allows a more detailed level of phenotypic description and is expected to improve drug discovery and target prediction. This principle is referred to as behavioral barcoding and has been previously described.[3]

Authors' Note

Underlying research materials of this study can be requested through the corresponding author.

Declaration of Conflicting Interests

The authors declared no potential conflicts of interest with respect to the research, authorship, and/or publication of this article. Thorsten Meinl and Michael R. Berthold have a financial interest in the company supporting the KNIME software. However, the generation of the automated workflow for PMR analysis was done for research purposes only and thus the workflow is made freely accessible.

Funding

The authors disclosed receipt of the following financial support for the research, authorship, and/or publication of this article: Matthijs van Leeuwen is supported by a postdoctoral fellowship of the Research Foundation Flanders (FWO).

References

1. Kokel, D.; Bryan, J.; Laggner, C.; et al. Rapid Behavior-Based Identification of Neuroactive Small Molecules in the Zebrafish. *Nat. Chem. Biol*. **2010**, *6*, 231–237.
2. Berthold, M. R.; Cebron, N.; Dill, F.; et al. KNIME—The Konstanz Information Miner. *SIGKDD Explor*. **2009**, *11*, 26–31.
3. Kokel, D.; Rennekamp, A. J.; Shah, A. H.; et al. Behavioral Barcoding in the Cloud: Embracing Data-Intensive Digital Phenotyping in Neuropharmacology. *Trends Biotechnol*. **2012**, *30*, 421–425.
4. Rihel, J.; Schier, A. Behavioral Screening for Neuroactive Drugs in Zebrafish. *Dev. Neurobiol*. **2012**, *72*, 373–385.
5. Kokel, D.; Dunn, T. W.; Ahrens, M. B.; et al. Identification of Nonvisual Photomotor Response Cells in the Vertebrate Hindbrain. *J. Neurosci*. **2013**, *33*, 3834–3843.
6. Wullimann, M. F. Secondary Neurogenesis and Telencephalic Organization in Zebrafish and Mice: A Brief Review. *Integr. Zool*. **2009**, *4*, 123–133.
7. Higashijima, S. I.; Schaefer, M.; Fetcho, J. R. Neurotransmitter Properties of Spinal Interneurons in Embryonic and Larval Zebrafish. *J. Comp. Neurol*. **2004**, *480*, 19–37.
8. Saint-Amant, L. Development of Motor Rhythms in Zebrafish Embryos. In *Progress in Brain Research*; Elsevier, **2010**; Vol. 187, pp 47–61.
9. McLean, D. L.; Fetcho, J. R. Ontogeny and Innervation Patterns of Dopaminergic, Noradrenergic, and Serotonergic Neurons in Larval Zebrafish. *J. Comp. Neurol*. **2004**, *480*, 38–56.
10. Holzschuh, J.; Ryu, S.; Aberger, F.; et al. Dopamine Transporter Expression Distinguishes Dopaminergic Neurons from Other Catecholaminergic Neurons in the Developing Zebrafish Embryo. *Mech. Dev*. **2001**, *101*, 237–243.
11. Sanchez-Simon, F. M.; Rodriguez, R. E. Developmental Expression and Distribution of Opioid Receptors in Zebrafish. *Neuroscience* **2008**, *151*, 129–137.
12. Gonzalez-Nunez, V.; Rodríguez, R. E. The Zebrafish: A Model to Study the Endogenous Mechanisms of Pain. *ILAR J*. **2009**, *50*, 373–386.
13. Boehmler, W.; Petko, J.; Woll, M.; et al. Identification of Zebrafish A2 Adenosine Receptors and Expression in Developing Embryos. *Gene Expr. Patterns* **2009**, *9*, 144–151.
14. Norton, W.; Rohr, K.; Burnstock, G. Embryonic Expression of a P2X3 Receptor Encoding Gene in Zebrafish. *Mech. Dev*. **2000**, *99*, 149–152.
15. Kucenas, S.; Li, Z.; Cox, J. A.; et al. Molecular Characterization of the Zebrafish P2X Receptor Subunit Gene Family. *Neuroscience* **2003**, *121*, 935–945.
16. Danilova, N.; Krupnik, V. E.; Sugden, D.; et al. Melatonin Stimulates Cell Proliferation in Zebrafish Embryo and Accelerates Its Development. *FASEB J*. **2004**, *18*, 751–753.
17. Eriksson, K. S.; Peitsaro, N.; Karlstedt, K.; et al. Development of the Histaminergic Neurons and Expression of Histidine Decarboxylase mRNA in the Zebrafish Brain in the Absence of All Peripheral Histaminergic Systems. *Eur. J. Neurosci*. **1998**, *10*, 3799–3812.
18. Peitsaro, N.; Sundvik, M.; Anichtchik, O. V.; et al. Identification of Zebrafish Histamine H1, H2 and H3 Receptors and Effects of Histaminergic Ligands on Behavior. *Biochem. Pharmacol*. **2007**, *73*, 1205–1214.
19. Moritz, C.; Berardi, F.; Abate, C.; et al. Live Imaging Reveals a New Role for the Sigma-1 (σ1) Receptor in Allowing Microglia to Leave Brain Injuries. *Neurosci. Lett*. **2015**, *591*, 13–18.
20. Rihel, J.; Prober, D. A.; Arvanites, A.; et al. Zebrafish Behavioral Profiling Links Drugs to Biological Targets and Rest/Wake Regulation. *Science* **2010**, *327*, 348–351.